Chapter 5

Towards Vessel Reconstruction from IVUS Data.

5.0.1 Methodology

In order to obtain experimental vessel wall morpho-geometric measures, an IVUS pullback of 2090 images corresponding to 45 mm long vessel segment from a pathological right coronary artery (See Fig. 4.2) was obtained. The sequence was acquired using a Boston Sci. equipment at 40 MHz at constant pullback speed of 0.5 mm/sec and segmented using the Neural Network procedure described in section 4.3.1. All geometric parameters have been obtained from an elliptical fitting to the vessel wall point find out by the Neural Network made it using the procedure described by [52].

Model Assumption.

One of the nice advantages of the proposed approach consists of providing a way to obtain a 2.5D reconstruction of the vessel wall. The experimental analysis, has demonstrated that it is possible to separate the geometric vessel properties from heart dynamics contributions (See Chapter 4). We assume that the vessel wall shape $\gamma = (x, y, z)$ at time t from catheter point of view, can be written as an elliptical approximation given by (See section 4.2):

$$x(t) = a(t)cos(\theta + \delta(t)) + cx(t)\ ,\ y(t) = b(t)sin(\theta + \delta(t)) + cy(t)\ ,\ z(t) = c_z(t); \quad (5.1)$$

where $(0 < \theta \leq 2\pi)$, determines the angular position of the corresponding point on the ellipse, $(a(t), b(t))$ are the minor and major radii of the ellipse, given by (Eq. 5.2), $\delta(t)$ is its orientation and $C = (cx(t), cy(t), c_z(t))$ its center at time t. In $2.5D$ IVUS reconstruction $c_z(t)$ is unknown, but in our model we can take it as the catheter position in longitudinal direction, $c_z = vt$, where v is the catheter velocity. Taking into account only the geometrical contributions, an approximated vessel geometry description from catheter point of view is possible, when lumen center position major and minor ellipses radii and the ellipses orientation are known.

Parameters Evolution.

In order to reconstruct the vessel wall from catheter point of view the principal ellipses temporal evolution parameters will be used.

1. **Minor and Major Axis**. The functional dependence between ellipse eccentricity ϵ and ellipses axis (see Eq. (4.9)), can be used to modell the temporal behavior of a(t) and b(t) (see Figures 5.1 and 5.2), as follows:

$$a(t) = a_g(t) + a_d(t) \quad , \quad b(t) = b_g(t) + b_d(t) \tag{5.2}$$

   where ($a_g(t)$,$b_g(t)$) and ($a_d(t), b_d(t)$) are the major and minor geometrical and dynamical ellipses axis temporal evolution. These contributions are given as a Fourier series:

$$a_g(t) = \sum_{n=n_1}^{n=n_2} \left(A_n^a cos(n\omega t) + B_n^a sin(n\omega t) \right) \tag{5.3}$$

$$b_g(t) = \sum_{n=n_1}^{n=n_2} \left(C_n^b cos(n\omega t) + D_n^b sin(n\omega t) \right) \tag{5.4}$$

$$a_d(t) = \sum_{n=n_3}^{n=n_4} \left(A_n^a cos(n\omega t) + B_n^a sin(n\omega t) \right)$$

$$b_d(t) = \sum_{n=n_3}^{n=n_4} \left(C_n^b cos(n\omega t) + D_n^b sin(n\omega t) \right)$$

2. **Ellipse Orientation** The ellipse orientation $\delta(t)$ shows a bimodal behavior such as illustrated in Fig 5.3. The temporal dependence can be written as follows:

$$\delta(t) = \delta_g(t) + \delta_d(t) \tag{5.5}$$

   where ($\delta_g(t)$,$\delta_d(t)$) are the geometric and dynamical dependence respectively. These contributions can be written as a Fourier series:

$$\delta_g(t) = \sum_{n=n_1}^{n=n_2} \left(A_n^\delta cos(n\omega t) + B_n^\delta sin(n\omega t) \right) \tag{5.6}$$

$$\delta_d(t) = \sum_{n=n_3}^{n=n_4} \left(A_n^\delta cos(n\omega t) + B_n^\delta sin(n\omega t) \right)$$

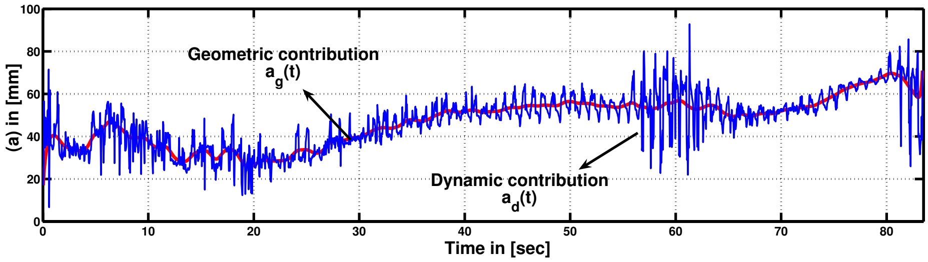

(a)

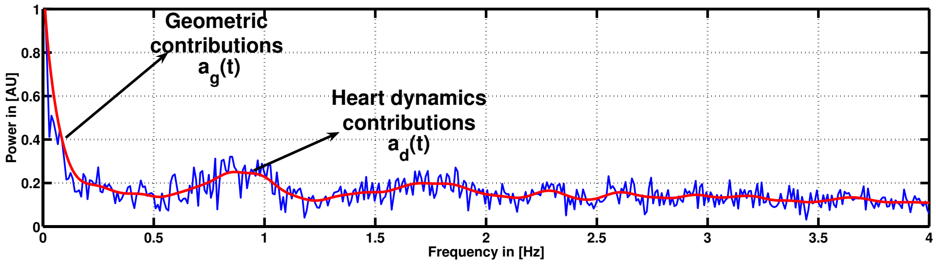

(b)

Figure 5.1: Major $a(t)$ ellipses axis temporal evolution (a) and its corresponding power spectral density (b)

3. **Ellipses Center.** The coordinates ellipse centers $cx(t)$ and $cy(t)$ follow a periodic bimodal movement (see Figures 5.4 (a) and 5.5 (a)). Their spectral density shows that there is a bimodal behavior which comes from geometric and dynamical contributions (See Figures. 5.4 (b) and 5.5 (b)). Using these results we can write the ellipse centers temporal evolution as follows:

$$cx(t) = cx_g(t) + cx_d(t) \quad , \quad cy(t) = cy_g(t) + cy_d(t) \tag{5.7}$$

where $(cx_g(t)$,$cy_g(t))$ and $(cx_d(t), cy_d(t))$ are the geometrical and dynamical ellipse center temporal contributions. These contributions are given as a Fourier series:

$$cx_g(t) = \sum_{n=n_1}^{n=n_2} \left(A_n^c cos(n\omega t) + B_n^c sin(n\omega t)\right) \tag{5.8}$$

$$cy_g(t) = \sum_{n=n_1}^{n=n_2} \left(C_n^c cos(n\omega t) + D_n^c sin(n\omega t)\right) \tag{5.9}$$

$$cx_d(t) = \sum_{n=n_3}^{n=n_4} \left(A_n^c cos(n\omega t) + B_n^c sin(n\omega t)\right)$$

$$cy_d(t) = \sum_{n=n_3}^{n=n_4} \left(C_n^c cos(n\omega t) + D_n^c sin(n\omega t)\right)$$

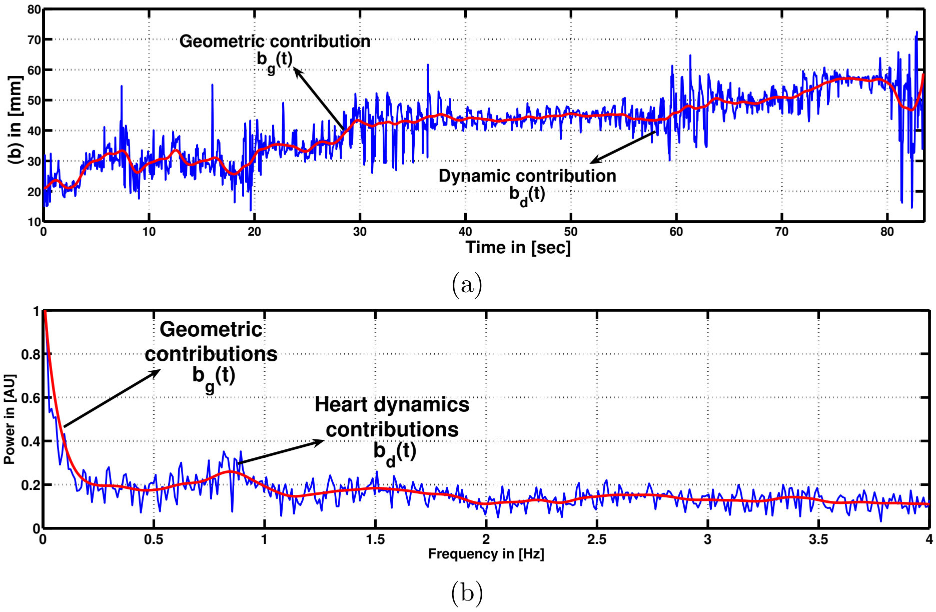

Figure 5.2: Minor $b(t)$ ellipses axis temporal evolution (a) and its corresponding power spectral density (b).

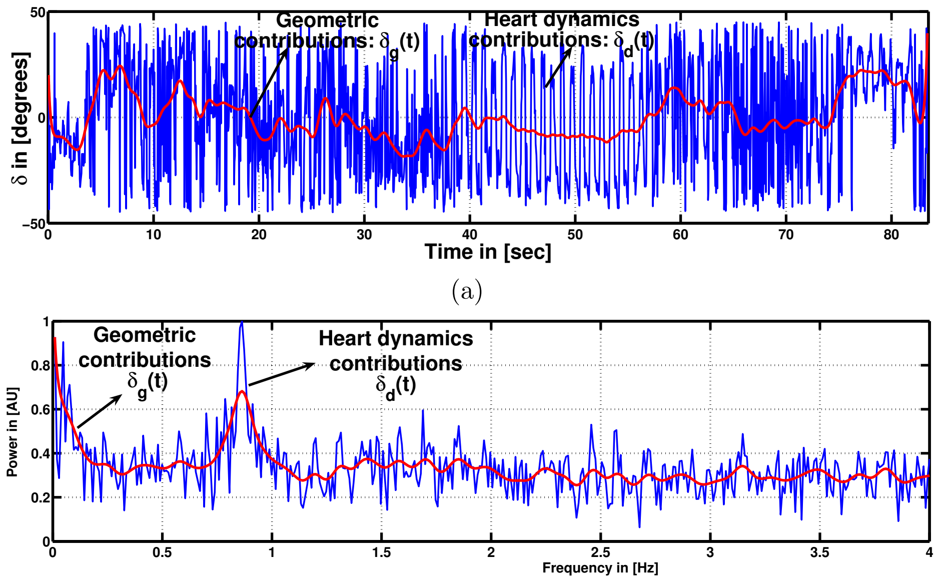

Figure 5.3: Ellipse orientation δ temporal evolution (a) and its corresponding power spectral density (b).

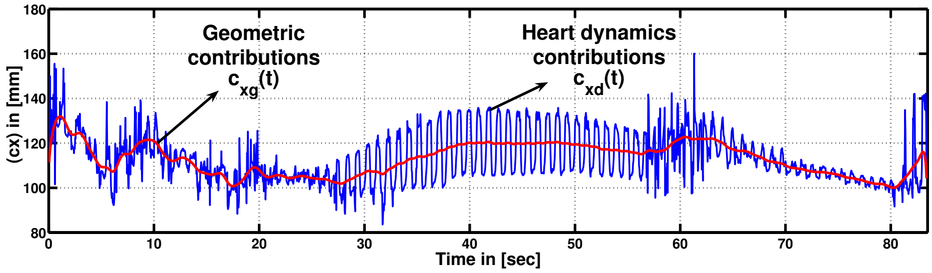

(a)

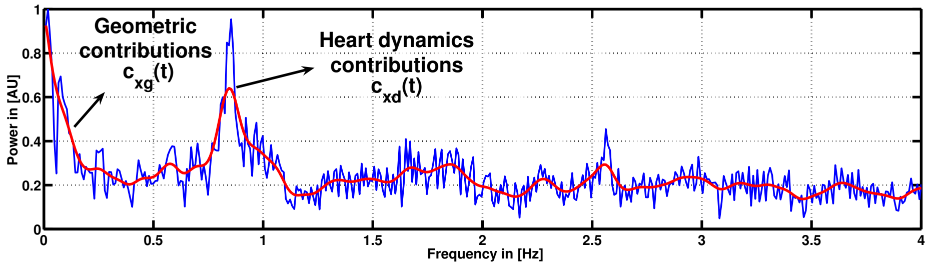

(b)

Figure 5.4: Ellipse center $cx(t)$ temporal evolution (a) and its corresponding spectral density (b)

The Fourier coefficients (A_n, B_n, C_n, D_n) in the range interval $[n_1, n_2]$ for geometrical contributions and $[n_3, n_4]$ for dynamical contributions, are obtained from the temporal evolution analysis of each dynamic parameter.

5.1 2.5D Vessel Reconstruction.

The 2.5D vessel reconstruction is possible taking only the Fourier coefficient that corresponds to the geometrical contribution. Therefore, Eq. 5.10 can be rewritten as follows:

$$\begin{aligned} x(t) &= a_g(t)cos(\theta + \delta_g(t)) + cx_g(t) \\ y(t) &= b_g(t)sin(\theta + \delta_g(t)) + cy_g(t) \\ z(t) &= vt \end{aligned}$$

where $(0 < \theta \leq 2\pi)$ determines the angular position of the corresponding point on the ellipse, $(a_g(t), b_g(t), \delta_g, cx_g, cy_g)$ are the minor and major axis radii, orientation, ellipse centers at time t and $v = 0.5$ mm/s the catheter velocity.
Figure 5.6 shows two views of a 2.5D vessel reconstruction of an IVUS pullback of 2090 images corresponding to 45 mm long vessel segment before rotation suppression and (Fig. 5.7) display two views of the same vessel when the dynamics suppression methodology has been applied.

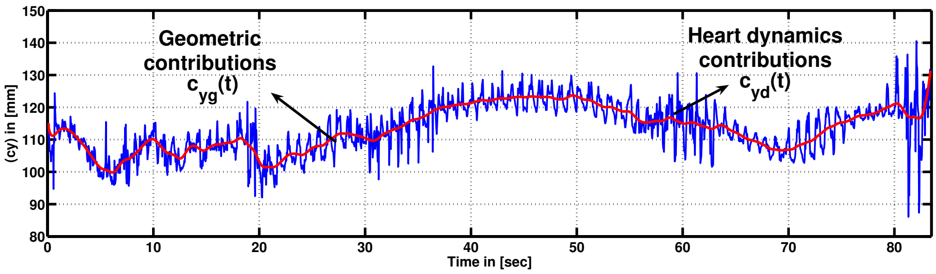

(a)

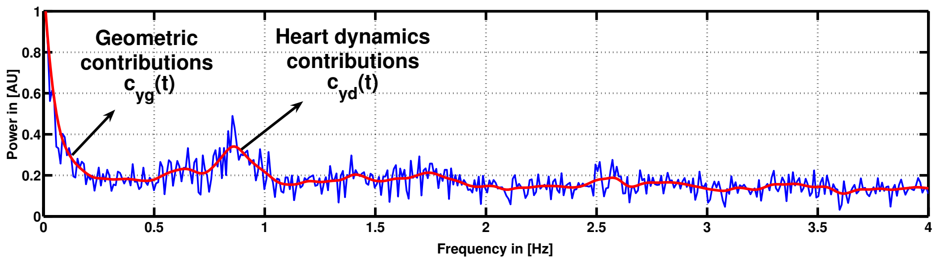

(b)

Figure 5.5: Ellipse center $c_y(t)$ temporal evolution (a) and its corresponding spectral density (b)

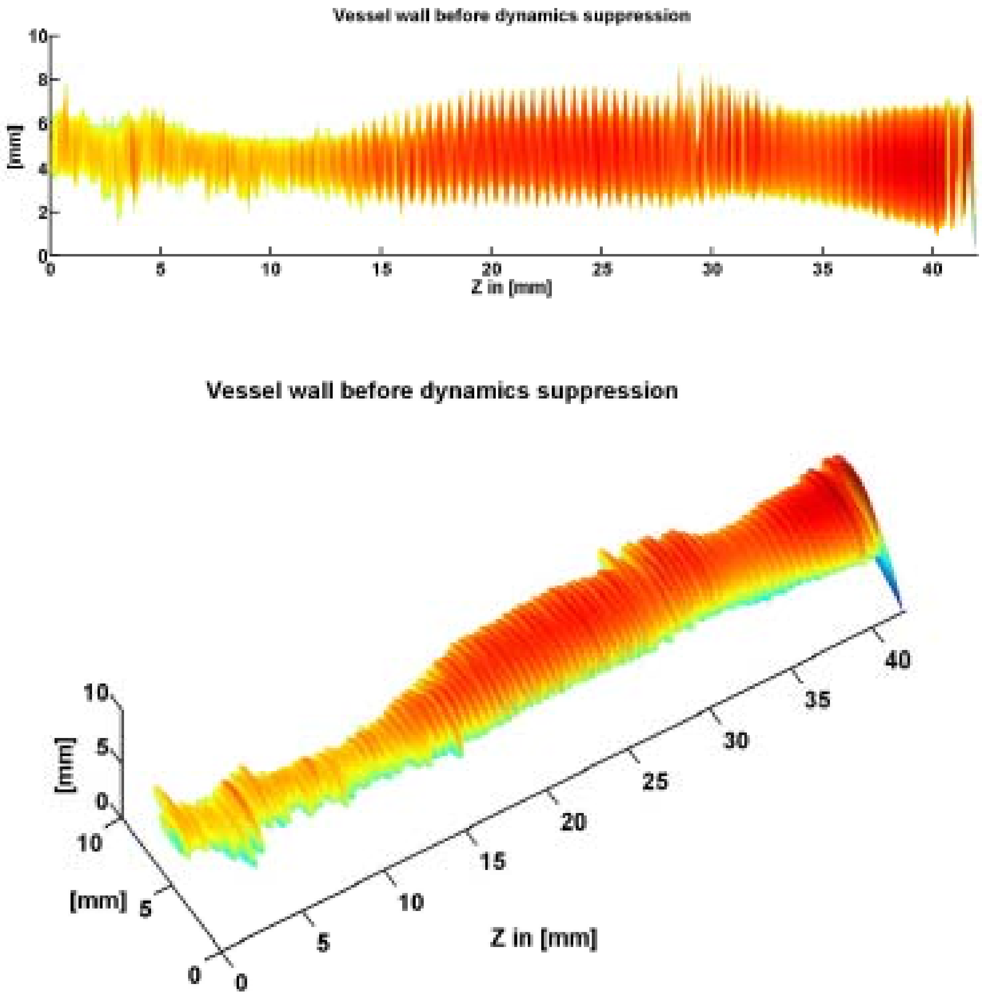

Figure 5.6: Two views of 2.5D vessel wall reconstruction before dynamic suppression.

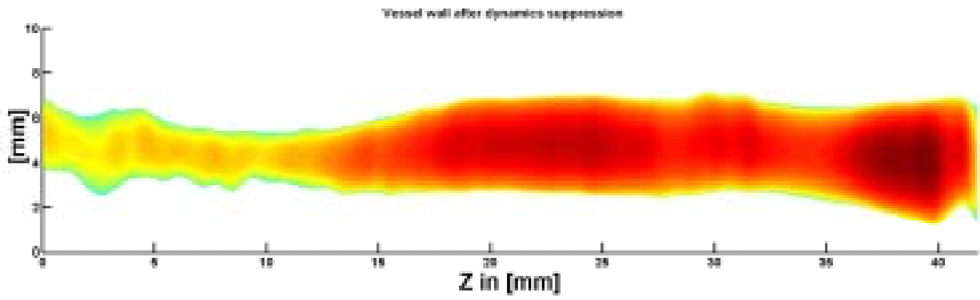

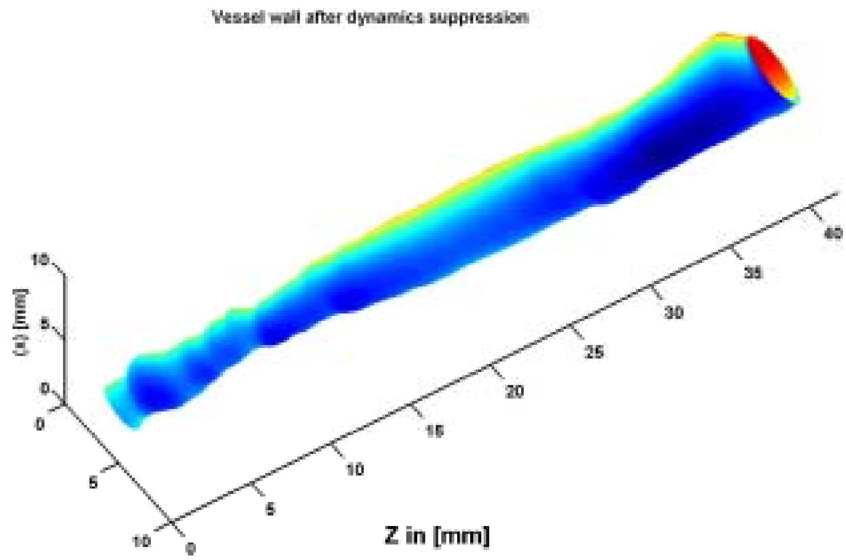

Figure 5.7: Two views of 2.5D vessel wall reconstruction after dynamic suppression.

Chapter 6

Conclusions and Future Lines

Although IVUS is continuously gaining its use in practice due to its multiple clinical advantages, the technical process of IVUS image generation, geometrical and dynamical aspect of the vessel wall evolution are not known by doctors and researchers developing IVUS image analysis. We developed in this thesis three complementary research studies: First one, we created a basic simulation model in order to generate 2D IVUS images. Second one, based on experimental results we introduced a new methodology to study the vessel wall appearance and its corresponding temporal evolution. Third, we introduced the main conceptual strategy that allows the 2.5D IVUS reconstruction.

1. *IVUS Images Simulation Model.* We discussed a basic physical model to generate synthetic 2D IVUS images. The model has different utilities: Firstly, expert can generate simulated IVUS images in order to observe different arterial structures of clinical interest and their grey level distribution in real images. Secondly, researchers and doctors can use our model to learn and to compare the influence of different physical parameters in the IVUS image formation, for example: the ultrasound frequency, the attenuation coefficient, the beam number influence, and the artifact generations. Third, this model can generate large database of synthetic data under different devices and acquisition parameters to be used to validate the robustness of image processing techniques. The IVUS image generation model provides a basic methodology that allows to observe the most important real image emulation aspects. This initial phase does not have the intention to compare pixel to pixel values generation, showing the coincidence with the real image, but looks for a global comparison method based on grey level difference distribution. The input model applies standard parameters that have been extracted from the literature. Hence this model is generic in terms that the model allows simulating different processes, parameters, and makes possible to compare to real data and to justify the generated data from the technical point of view.
   The model is based on the interaction of the ultrasound waves with a discrete

scatterer distribution of the main arterial structures. The obtained results of the validation of our model illustrate a good approximation to the image formation process. The 2D IVUS images show a good correspondence between the arterial structures that generate the image structures and their grey level values. The simulations of the regions and tissue transitions of interest lumen and adventitia, have been achieved in a satisfactory degree. Interested readers are invited to check the generation model in (http://www.cvc.uab.es/∼misael).

2. *Modelling Vessel Wall Dynamics.* We developed a geometric and kinematic model in order to study the evolution of coronary artery wall from catheter point of view. The model is based on the supposition that the evolution of the arterial wall, can be modelled assuming two principal contributions that come from different physical reasons. The first one, a systematic contribution caused by geometric intrinsic arterial properties and the second one, an oscillating contribution that comes from ventricle dynamics. These contributions govern in major degree the profiles appearance of arterial wall in longitudinal views. Using these assumption we generate the methodological strategy in order to estimate and suppress IVUS dynamical distortions.
The vessel wall radial deformation on the IVUS images not only depends on the blood pressure variation, but also depends on the artifact produced by oscillating obliquity induced by the ventricle pulsatile dynamics. Any effort to obtain in situ vessel wall elastic properties using IVUS sequences should emphasize on the suppression of radial deformation that are blood pressure independent. We introduce a new conceptual formulation that permits to separate geometric contribution depending on intrinsical vessel wall micro-architecture from dynamical contribution that comes from heart movement. Our model only takes into account those transformations that maintain invariant the image dimensions, therefore the radial expansion and the catheter obliquity have not been treated, still these contributions predominate once suppressed the rotation.

3. *2.5D Vessel Reconstruction.* Being possible to separate the geometric contribution from dynamics contribution, we developed the basis to $2.5D$ vessel reconstruction only using IVUS data. This thesis gives an important advance in vessel wall dynamics estimation such as to introduce an alternative technique to estimate local heart dynamics. In this way, we provide a new possibility of studying robustly the vessel dynamics and establishing new diagnostic tools.

6.1 Future Lines

An important future line in this research can be oriented to IVUS Functional Image. The principal objective in this investigation way should be focused to find significative statistical correlation between static and dynamica morpho-geometric IVUS parameters and their corresponding cardiological functional dependence. In order to fulfill this general objective, the following research aspect can be consider as plausible:

1. Once separated the heart dynamics influence from geometric vessel wall contributions, we can characterize vessel wall mechanical properties evaluating the elastic constant σ_k extracted from the relative radial deformation $\Delta R_k/R_k$ for each frame k. This technique can be a novel and direct method to obtain plaque and tissue characterization by patient *in vivo*.

2. Using IVUS technique by frequencies greater than 40 MHz it is possible to observe the fibers configuration in cross sectional images. An exhaustive study of IVUS images textural properties, could be used to estimate the fiber density, allowing to obtain intrinsical properties of vessel wall, that can give an important valuation on functional and local physiological state of an artery.

3. Our dynamical and geometric model can be used in two ways: 1.- Suppression of dynamical distortion in order to obtain 3D IVUS reconstruction. 2.- Once suppressed the dynamics effect, *in vivo* vessel wall elastic properties can be estimated. 3.- Parameters validation that can be used to estimate heart dynamics.

4. The IVUS rotation as a global phenomena can be used to evaluate the pumping heart percentage efficiency. An extensive study of the IVUS rotation images versus pumping heart efficiency obtained experimentally using a diastolic and systolic angiography heart views, should demonstrate a positive correlation between heart rotation and heart efficiency.

Appendix A

Eccentricity Definition

In order to describe the IVUS rotation effect respect to the catheter spatial position, we define from (Fig. A.1 (a)) the catheter eccentricity as: $\xi = |rc_1/r|$, where $rc_1 =$

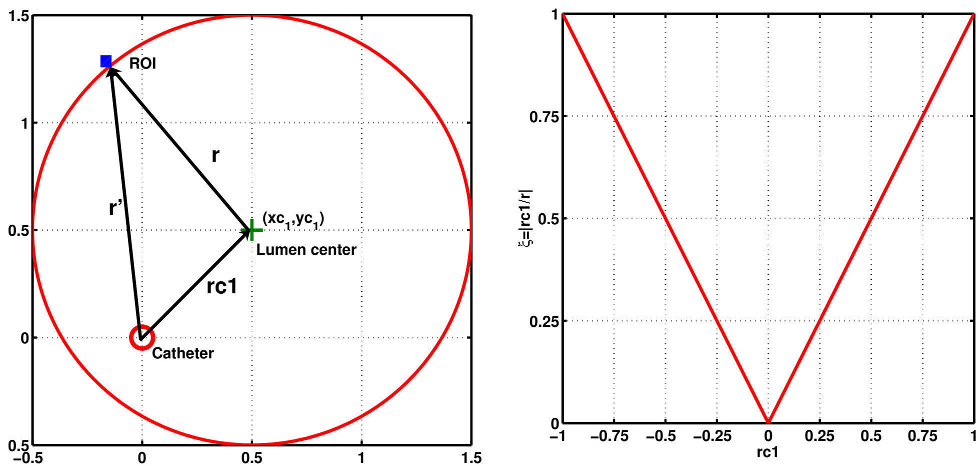

(a) (b)

Figure A.1: Catheter eccentricity ξ geometric definitions (a) ξ vs lumen center spatial position rc_1 (b)

$(xc_1^2 + yc_1^2)^{1/2}$ is the spatial relative catheter position to the lumen center and r is a region of interest (ROI) located on the vessel wall. Figure A.1 (b) shows the linear dependence of eccentricity ξ versus lumen center spatial position, rc_1. The definition of catheter eccentricity ξ can be used to achieve a better description of the heart dynamics influence and vessel geometry contributions to the longitudinal IVUS cuts' shape appearance.

Appendix B

Kinematic Approach to IVUS Rotation Estimation.

In order to find the rotation profile of the sequence when $0 \leq \xi \leq 10\%$, we assume [27] that the vessel wall can be consider as a discrete linear elastic oscillating system [19]. Using polar coordinates to describe the vessel wall temporal evolution, it follows that its trajectory is given by: $(x, y) = (r(t)cos(\theta(t)), r(t)sin(\theta(t)))$, then an element of the vessel wall has the following total energy:

$$E_i = T_i + U_i \tag{B.1}$$

$$where \qquad T_i = \frac{m_i v_i^2}{2} + \frac{m_i}{2}(r_i\omega_i)^2 \qquad U_i = \frac{k_i r_i^2}{2}$$

$$v_i = \sqrt{vx_i^2 + vy_i^2} \qquad r_i = \sqrt{x_i^2 + y_i^2} \qquad w_i = \frac{\partial\theta_i}{\partial t}$$

T_i and U_i, are the kinetic and elastic energy of the i-th discrete element of the vessel wall respectively, m_i,v_i, ω_i and k_i are the mass, tangential velocity, angular velocity and elasticity constant of the i-th element of the vessel wall. The mass of one element can be estimated considering the minimal "voxel" volume sweeping by the ultrasound beam, being this $V_b \approx 6.4 \times 10^{-5}\ mm^3$ [51]. Using this fact, the element of mass is $m = \rho * V_b \approx 1.09\frac{grs}{cm^3} * 6.4 \times 10 - 8grs \approx 6.97 \times 10^{-5}kg$, where ρ is the typical tissue density [48]. Within the above kinematic framework, it is sufficient to provide the temporal evolution of a single point on the vessel wall structure [42, 44], to measure the angular difference between two consecutive frames. Therefore, spatial location of this reference point was determined as the position ij of the vessel wall that has a minimal total energy given by (Eq. B). The spatial location of this point is put into the image spatial coordinates which reaches the condition:

$$(x_c, y_c) = argmin_{ij} \sum_{k=1}^{f_n} E_{ij}^k$$

where $f_n = 25$ is the image number used to evaluate this condition and ij are the row an columns of the average IVUS images.

Appendix C

Vessel and Ventricle Dynamic Interaction

The spatial-time evolution of an artery which is modelled for a generatrix curve G(s,t), is governed by the left ventricle (LV) evolution model specified in [40] (See Appendix C). The basic geometric model is given in a prolate sphere, whose parameters are shown in (Fig. C.1 (a)). A point (λ, η, ϕ) in prolate spheroidal coordinates has the

Figure C.1: Prolate coordinates (a) used to represent the LV surface (b)

following Cartesian coordinates:

$$x = \delta sinh\lambda sin(\eta)cos(\phi)\ ,\ y = \delta sinh\lambda sin(\eta)sin(\phi)\ ,\ z = \delta cosh\lambda cos(\eta)$$

where (λ, η, ϕ) are the radius, elevation and azimuthal angles respectively and δ is the focal radius. The evolution spatial and temporal of the generatrix curve $G(s,t)$ can be rewritten as a function of the curve $g(u(\lambda,\phi,\eta), v(\lambda,\phi,\eta), w(\lambda,\phi,\eta))$ on the surface of the prolate sphere, as follow:

$$G(s(\lambda,\phi,\eta),t) = gx(s(u(\lambda,\phi,\eta)),t) + gy(s(v(\lambda,\phi,\eta)),t) + gz(s(w(\lambda,\phi,\eta)),t) \quad \text{(C.1)}$$

The general matrix equation that transform one point $G(s,t)$ in $G(s+\delta s, t+\delta t)$ on the surface of the ventricle is given as:

$$G(s+\delta s, t+\delta t) = FaF6F5F4F3F2F1FoG(s,t) \quad \text{(C.2)}$$

$$Fo = \begin{pmatrix} a^{1/3} & 0 & 0 & 0 \\ 0 & a^{1/3} & 0 & 0 \\ 0 & 0 & a^{1/3} & 0 \\ 0 & 0 & 0 & a^{1/3} \end{pmatrix} \quad F1 = \begin{pmatrix} \varepsilon & 0 & 0 & 0 \\ 0 & \varepsilon & 0 & 0 \\ 0 & 0 & \varepsilon & 0 \\ 0 & 0 & 0 & \varepsilon \end{pmatrix}$$

$$F2 = \begin{pmatrix} cos(b)/|r1| & -sin(b)/|r1| & 0 & 0 \\ sin(b)/|r1| & cos(b)/|r1| & 0 & 0 \\ 0 & 0 & 1 & 0 \\ 0 & 0 & 0 & 1 \end{pmatrix}$$

where a is the correctional parameter that transform a prolate spheroidal shell into a more spherical shape in anticipation of the next transformation, $\epsilon = \left(1 + \frac{3k_1V_w}{4\pi|FoG(s,t)|}\right)^{1/3}$, V_w is the wall ventricle volume, in our model $V_w = 1$, $b = ak_2z1$ and $r1 = F1FoG(s,t) = [x_1, y_1, z_1, 1]^t$

$$F3 = \begin{pmatrix} a^{-1/3}exp(k_4 - (k_3/2)) & 0 & 0 & 0 \\ 0 & a^{-1/3}exp(k_4 - (k_3/2)) & 0 & 0 \\ 0 & 0 & a^{2/3}exp(k_3) & 0 \\ 0 & 0 & 0 & a^{-1/3} \end{pmatrix}$$

$$F4 = \begin{pmatrix} 1 & k_5 & 0 & 0 \\ k_5 & 1+k_5^2 & 0 & 0 \\ 0 & 0 & 1 & 0 \\ 0 & 0 & 0 & 1 \end{pmatrix} \quad F5 = \begin{pmatrix} 1 & 0 & k_6 & 0 \\ 0 & 1 & 0 & 0 \\ k_6 & 0 & 1+k_6^2 & 0 \\ 0 & 0 & 0 & 1 \end{pmatrix} \quad F6 = \begin{pmatrix} 1 & 0 & 0 & 0 \\ 0 & 1 & k_7 & 0 \\ 0 & k_7 & 1+k_7^2 & 0 \\ 0 & 0 & 0 & 1 \end{pmatrix}$$

$Fa = A4A3A2A1$

$$A1 = \begin{pmatrix} 1 & 0 & 0 & 0 \\ 0 & cos(k_8) & -sin(k_8 & 0 \\ 0 & sin(k_8) & cos(k_8 & 0 \\ 0 & 0 & 0 & 1 \end{pmatrix} \quad A2 = \begin{pmatrix} cos(k_9) & 0 & sin(k_9 & 0 \\ 0 & 1 & 0 & 0 \\ -sin(k_9 & 0 & cos(k_9 & 0 \\ 0 & 0 & 0 & 1 \end{pmatrix}$$

$$A3 = \begin{pmatrix} cos(k_{10}) & -sin(k_{10}) & 0 & 0 \\ sin(k_{10}) & cos(k_{10}) & 0 & 0 \\ 0 & 0 & 1 & 0 \\ 0 & 0 & 0 & 1 \end{pmatrix}$$

$$A4 = \begin{pmatrix} 1 & 0 & 0 & k_{11} \\ 0 & 1 & 0 & k_{12} \\ 0 & 0 & 1 & k_{13} \\ 0 & 0 & 0 & 1 \end{pmatrix}$$

$\mathbf{k}_i$	**Dependence**
k_1	Radially dependent compression
k_2	Left ventricular torsion
k_3	Ellipticallization in long axis plane
k_4	Ellipticallization in short axis plane
k_5	Shear in x direction
k_6	Shear in y direction
k_7	Shear in z direction
k_8	Rotation about x-axis
k_9	Rotation about y-axis
k_{10}	Rotation about z-axis
k_{11}	Translation in x direction
k_{12}	Translation in y direction
k_{13}	Translation in z direction

The temporal and spatial evolution of the ventricle surface is given by the evolution of the k_i parameters given in the model by Arts et al. [38]. Fig. C.2 show the temporal evolutions from k_1 to k_{13} for two cardiac cycles.

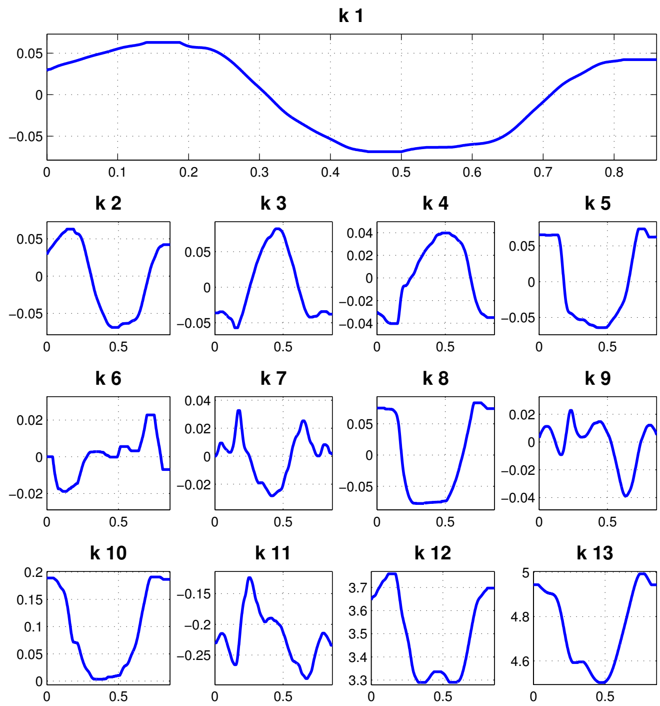

Figure C.2: The temporal evolution of k_i coefficients

Bibliography

[1] Heart Disease and Stroke Statistics 2005 Update, American Heart Association.

[2] Wahle A., Prause PM., DeJong SC, Sonka M. Geometrically correct 3-D reconstruction of intravascular ultrasound images by fusion with biplane angiographyMethods and validation. IEEE Trans Med Imaging 1999;18(8):686-699.

[3] Roelandt JRTC, Dimario C, Pandian NG, et al. Three-dimensional reconstruction of intracoronary ultrasound images: rationale, approaches, problems, and directions. Circulation. 1994;90:1044-1055

[4] Klein H-M, Gnther RW, Verlande M, et al. 3-D-surface reconstruction of intravascular ultrasound images using personal computer hardware and a motorized catheter control. In: Cardiovascular and Interventional Radiology. 1992;15:97-101

[5] Evans JL, Ng KH, Wiet SG, et al. Accurate three-dimensional reconstruction of intravascular ultrasound data: spatially correct three-dimensional reconstructions. Circulation. 1996;93:567-576.

[6] Laban M, Oomen JA, Slager CJ, et al. ANGUS: a new approach to three dimensional reconstruction of coronary vessels by combined use of angiography and intravascular ultrasound. In: Murray A, Arzbaecher R, eds. Computers in Cardiology. Piscataway, NJ: IEEE Computer Society; 1995:325-328

[7] Slager CJ, Wentzel JJ, Oomen JA, et al. True reconstruction of vessel geometry from combined x-ray angiographic and intracoronary ultrasound data. Semin Intervent Cardiol. 1997;2:43-47.

[8] Metz J., Paul G., Fitzgerald P., Intravascular Ultrasound Imaging, Jonathan M. Tobis y Paul G. Yock. Churchil Livinstone Inc., 1992.

[9] Yock P., Linker D., Saether O., et al., Intravascular two dimensional catheter ultrasound, Initial clinical studies, abstracted, Circulations, No. 78 (suppl II): II-21, 1988.

[10] Metz Jonas A., Paul G., Fitzgerald Peter J., Intravascular ultrasound basic interpretation, in Beyond Angiography, Intravascular Ultrasound, State of the art, Vol. XX, Congress of the ESC Viena-Austria, Stanford University School of Medicine, California, USA., 1998.

[11] Kearney P., Erbel R., Imaging in the characterization laboratory, in Beyond Angiography, Intra vascular Ultrasound, state of the art, Vol. XX, Congress of the ESC Viena-Austria, Johannes Gutenberg University, Mainz and University Clinic,Essen,Germany, 1998.

[12] Verhoef W. A., Cloostermans M. J., Thijssen J. M., The impulse response of a focused source with an arbitrary axisymmetric surface velocity distribution, Journal Acoustic Society American, Vol. 75, pp. 1717-1721, 1984.

[13] Fontaine I., Bertrand M, Cloutier G., A system-based approach to modelling the ultrasound signal backscattered by red blood cells,Biophysical Journal, Vol. 77, pp. 2387-2399, 1999

[14] Fan L., Herrington D., Santiago P., Simulation of b-mode ultrasound to determine features of vessel for image analysis,Computers in Cardiology, Vol. 25, pp. 165-168,1998

[15] Kinsler L. , Fundamentos de acústica, LIMUSA, Noriega Editores, 1995.

[16] Cheeke D., Fundamentals and Aplications of Ultrasonic Waves, CRC PRESS, 2002.

[17] Thijssen J, Oosterveld B., Perfomance of echographic equipment and potentials for tissue characterization, NATO ASI Series, Mathematics and Computer Science in Medical Imaging, Vol. F39, pp. 455-468, 1988.

[18] Zagzebski J., Essential of Ultrasound Physics, Mosby A. hardcourt Healt Sciences Company, 1996.

[19] Mazumdar J., Biofluids Mechanics, World Scientific Publishing, 1992.

[20] Shung and Thieme., Ultrasonic scatering in biological tissues, CRC Press, Boca Raton, Ann Arbor, London,Tokyo, 1993.

[21] Guyton A., Tratado de Fisiología Médica, Décima edición, Mcgraw-Hill Interamericana, 2001.

[22] Perelman L., and et al, Observation of periodic fine structure in reflectance from biological tissue: A new technique for measuring nuclear size distribution, Physical Review Letters, Vol. 80, No. 3, pp. 627-630, January 1998.

[23] Duda R., Hart P., Stork D., Pattern Clasification, Johon Wiley & sons, INC, 2000.

[24] Gonzales R., Wintz P., Digital Image Processing, Addison Wesley, 1987.

[25] O'Donnell M., Silverstein S., Optimum displacement for compound image generation in medical ultrasound, IEEE Transaction on Ultrasonics, Ferroelectrics and Frequency Control, Vol. 35, No. 4, pp. 470-476, 1988.

[26] Rosales M., Radeva P., Empirical simulation model of intravascular ultrasound, Tech. Rep., No. 71, Centre de Visió per Computador, Universitat Autónoma de Barcelona/España, 2003.

[27] Rosales M., Radeva P., et al. Suppression of IVUS Image Rotation. A Kinematic Approach, FIMH 2005, LNCS 3504, pp. 359 368, 2005. Springer-Verlag Berlin Heidelberg 2005

[28] Berry E., and et al, Intravascular ultrasound-guided interventions in coronary artery disease, NHS R D HTA Programme, 2000.

[29] G.A. Holzapfel, T.C. Gasser, R.W. Ogden, A new constitutive framework for arterial wall mechanics and a comparative study of material models. Biomech Preprint Serie, Paper No. 8 November 2000.

[30] Patrick H. W. Inteligencia Artificial, Addison Wesley Iberoamericana, 1994.

[31] Boston Scientific Corporation, Scimed division, The ABCs of IVUS, 1998.

[32] Vogt M., and et al, Strutural analysis of the skin using high frequency broadband ultrasound in the range from 30 to 140 MHz, IEEE Internationalk Ultrasonics Syposium, Sendai, Japan, 1998.

[33] Graham S., Brands D., and et al., Assesment of arterial wall morphology using intravascular ultrasound *in vitro* and in patient, Circulations, II-56, 1989.

[34] Jumbo G., Raimund E., Novel techniques of coronary artery imaging, in Beyond Angiography, Intra Vascular Ultrasound, state of the art, Vol. XX, Congress of the ESC Viena-Austria, University of Essen,Germany, 1998.

[35] Di Mario C., et al. The angle of incidence of the ultrasonic beam a critical factor for the image quality in intravascular ultrasonography. Am Heart J 1993;125:442-448.

[36] Zamir, M., The Physics of Pulsatile Flow Series: Biological and Medical Physics, Biomedical Engineering 2000, XVII, 220 p. 81 illus., Hardcover ISBN: 0-387-98925-0

[37] Hiroshi Yamada., Strength of biological materials., edited by, F. Gay Nor Evans, Baltimore, 1970;

[38] T. Arts et al, Description of the deformation of the left ventricle by a kynematic model. J. Biomechanics, 25(10): 1119-1127, 1992.

[39] Axel Jantsch, System modelingg: Model of computation and their applications, Royal Institute of Thecnology, Stockolm, Sweden, 2005

[40] Edo Waks., and etal, Cardiac Motion Simulator for Tagged MRI, Proceeding of MMBIA 1996, IEEE. John Hopkins University, Baltimore, MD 21218.

[41] Dirk Hausmann. MD, Andrea Jean, and et al, Intracoronary ultrasound imaging: Intraobserver and interobserver variability of morphometric measurements. Beyong Angiography, Intravascular Ultrasound, August 1998, XX Congress of ESC, Viena Austria.

[42] Kittel, C., Knight, W., Ruderman, M, Mechanics, Berkeley physics course, vol 1, Revert, 1991.

[43] Brian K., and et al, Effects of transducer position on backscatered intensity in coronary arteries. Ultrasound in medicine and Biology, Vol. 28, No 1, pp. 81-91, 2002.

[44] Broucke, R, Lagrangian and hamiltonian methods in the theory of rotational motion of a rigid body. IASOM TR-78-7. The University of Texas at Austin. 1978

[45] Arendt Jesen J., Linear Descripcion of Ultrasound Imaging System, Notes for the international Summer School on Advanced Ultrasound Imaging, Tecnical University of Denamark, 2001.

[46] Korte Chris L., Intravascular Ultrasound Elastography, Interuniversity Cardiology Institute of the Netherlands (ICIN), 1999.

[47] J. Declerck, N. Ayache, and E.R. McVeigh. Use of a 4D planispheric transformation for the tracking and the analysis of LV motion with tagged MR images. In SPIE Medical Imaging, vol. 3660, 1999

[48] Young B., and Heath J., Wheater's, Histología Funcional, 4ta edición, Ediciones Hardcourt, S.A, 2000.

[49] Bruining N, et al, ECG-gated versus nongated three-dimensional intracoronary ultrasound analysis: implications for volumetric measurements, Cathet Cardiovasc Diagn. 1998 Mar;43(3):254 - 60, Thoraxcenter, Department of Cardiology, Erasmus Medical Center and Erasmus University, Rotterdam, The Netherlands

[50] De Winter SA, et al, Retrospective image-based gating of intracoronary ultrasound images for improved quantitative analysis: the intelligate method, Catheter Cardiovasc Interv. 2004 Jan;61(1):84-94. Thoraxcentre, Department of Cardiology, Erasmus MC, Rotterdam, The Netherlands.

[51] Misael Rosales, Petia Radeva and et al. Simulation Model of Intravascular Ultrasound Images, Lecture Notes in Computer Science Publisher: Springer-Verlag Heidelberg, Medical Image Computing and Computer-Assisted Intervention MICCAI 2004, Volume 3217/ 2004, pp. 200-207, France, September, 2004.

[52] Andrew W. et al, Direct Least Square Fitting of Ellipses, IEEE Transactions on Pattern Analysis and Machine Intelligence, vol 21, number 5, p 476-480, 1999

[53] Williams MJ, et al. Assessment of the mechanical properties of coronary arteries using intravascular ultrasound: an *in vivo* study. Int J Card Imaging. 1999 Aug, 15(4):287-94.

[54] Seemantini K. Nadkarni, et al, Image-Based Cardiac Gating for Three- Dimensional Intravascular Ultrasound. Ultrasound in medicine and Biology, Vol. 31, No 1, pp. 53-63, 2005.

[55] De Micheli, E., and et al, The Accuracy of the Computation of Optical Flow and of the Recovery of Motion Parameters, IEEE Transactions on Pattern Analysis and Machine Intelligence, Vol. 15, No. 5, May 1993.

[56] Dodge JT, et al, Lumen diameter of normal human coronary arteries. Influence of age, sex, anatomic variation, and left ventricular hypertrophy or dilation. Department of Medicine, University of Washington, Seattle, Circulation. 1992 Jul;86(1):232-46.

[57] G. A. Holzapfel, et al, Biomechanical behavior of the arterial wall and its numerical characterization. Comp. Biol. Med., 28:377-392, 1998.

[58] J. D. Humphrey, Mechanics of arterial wall: Review and directions. Critical Reviews in Biomech. Engr., 23:1-162, 1995

[59] Seemantini K. Nadkarni, et al, A pulsating coronary vessel phantom for two- and three-dimensional intravascular ultrasound studies. Ultrasound in Medicine and Biology, Volume 29, Issue 4, April 2003, Pages 621-628

[60] Anderson W., et al, ACC Clinical Expert Consensus Document. American College of Cardiology Clinical Expert Consensus Document, Measurement and Reporting of IntraVascular Ultrasound Studies, Elsevier Science,Inc, 2001,No. 5,Vol. 37.

[61] Nissen SE. Application of intravascular ultrasound to characterize coronary artery disease and assess the progression or regression of atherosclerosis. Am J Cardiol 2002; 89(Suppl.):24B-31B.

[62] Giannattasio C, Failla M, Emanuelli G, et al. Local effects of atherosclerotic plaque on arterial distensibility. Hypertension 2001; 38(5) : 1177-1180.

[63] Di Mario C, von Birgelen C, Prati F, et al. Three dimensional reconstruction of cross sectional intracoronary ultrasound: Clinical or research tool Br Heart J 1995; 73 : 5(Suppl. 2) : 26-32.

[64] Delachartre P, Cachard C, Finet G, Gerfault FL, Vray D. Modeling geometric artefacts in intravascular ultrasound imaging. Ultrasound Med Biol 1999; 25(4) : 567-575.

[65] Roelandt JR, Di Mario C, Pandian NG, et al. Three-dimensional reconstruction of intracoronary ultrasound images. Rationale, approaches, problems, and directions. Circulation 1994;90(2) : 1044-1055.

[66] Thrush AJ, Bonnett DE, Elliott MR, Kutob SS, Evans DH. An evaluation of the potential and limitations of three-dimensional reconstructions from intravascular ultrasound images. Ultrasound Med Biol 1997; 23(3) : 437–445.

[67] Dijkstra J, Wahle A, Koning G, Reiber JHC, Sonka M. Quantitative coronary ultrasound: State of the art. What's New Cardiovascular Imaging 1998 : 79-94.

[68] Nissen SE, Yock P. Intravascular ultrasound: Novel pathophysiological insights and current clinical applications. Circulation 2001; 103(4): 604-616.

[69] Chris L. de Korte., Intravascular Ultrasound Elastography, Interuniversity Cardiology Institute of the Netherlands (ICIN), 1999.

[70] Evans JL., Ng KH., Wiet SG., et al. Accurate three - dimensional reconstruction of intravascular ultrasound data: Spatially correct three - dimensional reconstructions. Circulation 1996; 93(3) : 567–576.

[71] G.A. Holzapfel, T.C. Gasser, M. Stadler, A structural model for the viscoelastic behavior of arterial walls: Continuum formulation and finite element analysis, European Journal of Mechanics A-Solids Vol. 21 (2002) 441-463.

[72] Crick SJ, Sheppard MN, Ho SY, Gebstein L, Anderson RH. Anatomy of the pig heart: comparisons with normal human cardiac structure. J Anat. 1998 Jul;193:105-19.

Publications

- Empirical intravascular ultrasound simulation system. O Rodriguez Leor, J Mauri Ferre1, E Fernandez Nofrerias (1), E Tizon (2), A Tovar (1), V Valle Tudela1, M Rosales (2), P Radeva (2), Hospital Universitari Germans Trias i Pujol - Badalona - Spain, (1) HU Germans Trias i Pujol - Badalona - Spain, (2) Universitat Autonoma de Barcelona - Bellaterra - Spain, European Society of Cardiology Congress, Stokholm, Sweden, 3-7 sept 2005

- Misael Rosales, Petia Radeva, Debora Gil, Carlos Rodríguez and Oriol Rodríguez, Modelling of Image-Catheter Motion for 3-D IVUS. Medical Image Analysis, (Submitted 12/07/2005)

- Misael Rosales and Petia Radeva, Book Chapter: A Basic Model for IVUS Image Simulation. Handbook of Biomedical Image Analysis, Segmentation Models Part A Series, Suri, J.S.; Wilson, D.; Lakowicz, J.R.; Laximinarayan, S. (Eds.) 2005, XVIII, 648 p. 274 illus., ISBN: 0-306-48550-8

- Misael Rosales, Petia Radeva and Josepa Maury, Basic Model Of Simulation Of IVUS Data, (Part I: Model Exposition). Computerized Medical Imaging and Graphics, (Submitted 08/08/2004)

- Misael Rosales, Petia Radeva and Josepa Maury, Basic Model Of Simulation Of IVUS Data, (Part II: Model Validation). Computerized Medical Imaging and Graphics, (Submitted 08/08/2004)

- Rosales M., Radeva P., et al. Suppression of IVUS Image Rotation. A Kinematic Approach, FIMH 2005, LNCS 3504, pp. 359 368, 2005. Springer-Verlag Berlin Heidelberg 2005

- Rosales M., Radeva P., et al. Simulation Model of Intravascular Ultrasound Images, Lecture Notes in Computer Science Publisher: Springer-Verlag Heidelberg, Medical Image Computing and Computer-Assisted Intervention - MICCAI

2004, Volume 3217 / 2004, pp. 200-207, France, September, 2004.

- Oriol Pujol, Misael Rosales, Petia Radeva, et al, Intravascular Ultrasound Images Vessel Characterization Using AdaBoost. Lecture Notes in Computer Science Publisher, Springer-Verlag GmbH ISSN: 0302-9743, Volume 2674 / 2003, pp. 242 - 251.

- D. Rotger, M. Rosales, et al, ActiveVessel: A New Multimedia Workstation for IVUS and Angiography Fusion, Proceedings of Computers in Cardiology, 30:65-69, Thessaloniki, Greece, September, 2003.

- Modelo Físico para la Simulación de Imágenes de Ecografía Intracoronaria, Rodríguez O., Mauri J., Rosales Misael, Radeva Petia, Revista Espanola de Cardiología, 56(2), Congreso de las Enfermedades Cardiovasculares, Sevilla 10/2003

- Model Empíric de Simulació décografia Intravascular Rodríguez, O. Mauri, J. Fernández-Nofrerías, E Garcia, C. Villuendas, R. Tovar, A. Duran, A. Valle, V. Rosales, Misael Radeva, Petia, Revista Societat Catalana de Cardiología, 4(4):42, XIVé Congrés de la Societat Catalana de Cardiología, Barcelona —5—2003

- Empirical simulation model of intravascular ultrasound Rodríguez-Leor, O. Fernández-Nofrerías, E Mauri, J. Garcia, C. Villuendas, R. Valle, V. Rosales, Misael Radeva, Petia European Heart Journal, ESC Congress 2003, Vienna —1—2003

- Rosales M., Radeva P., Empirical simulation model of intravascular ultrasound, Tech. Rep., No. 71, Centre de Visió per Computador, Universitat Autónoma de Barcelona/España, 2003.